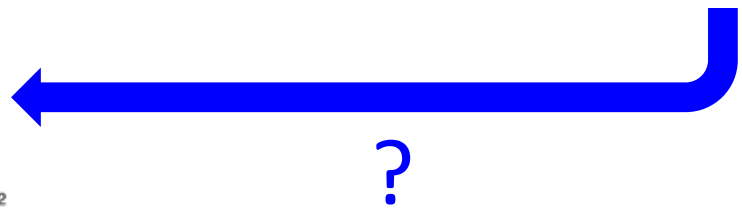
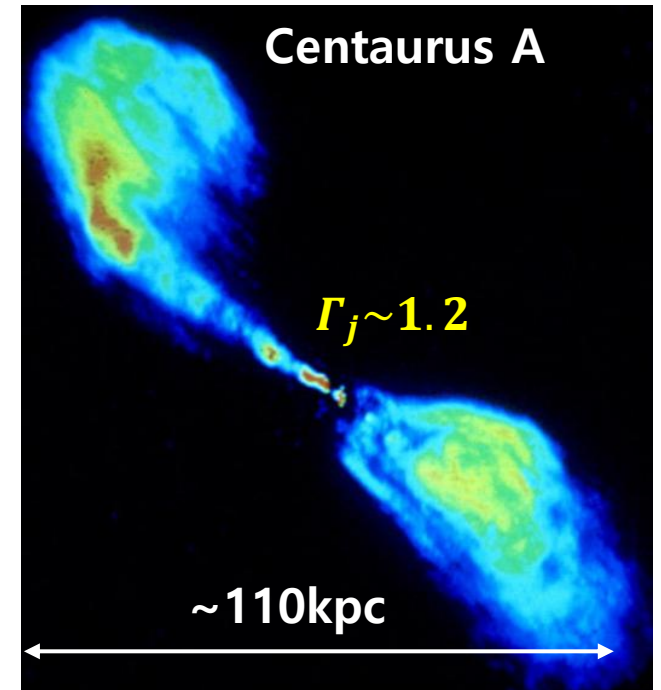
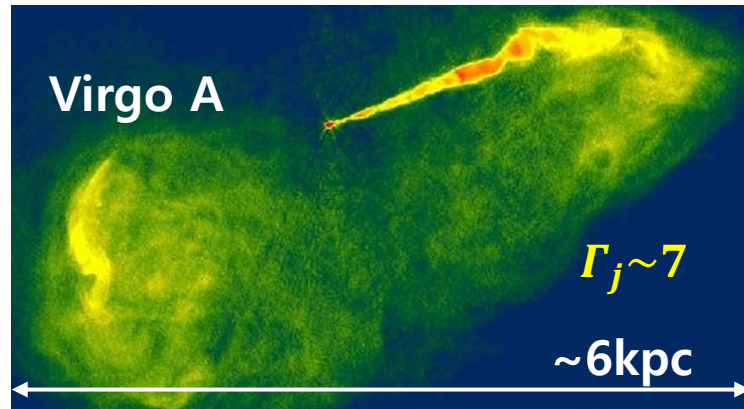
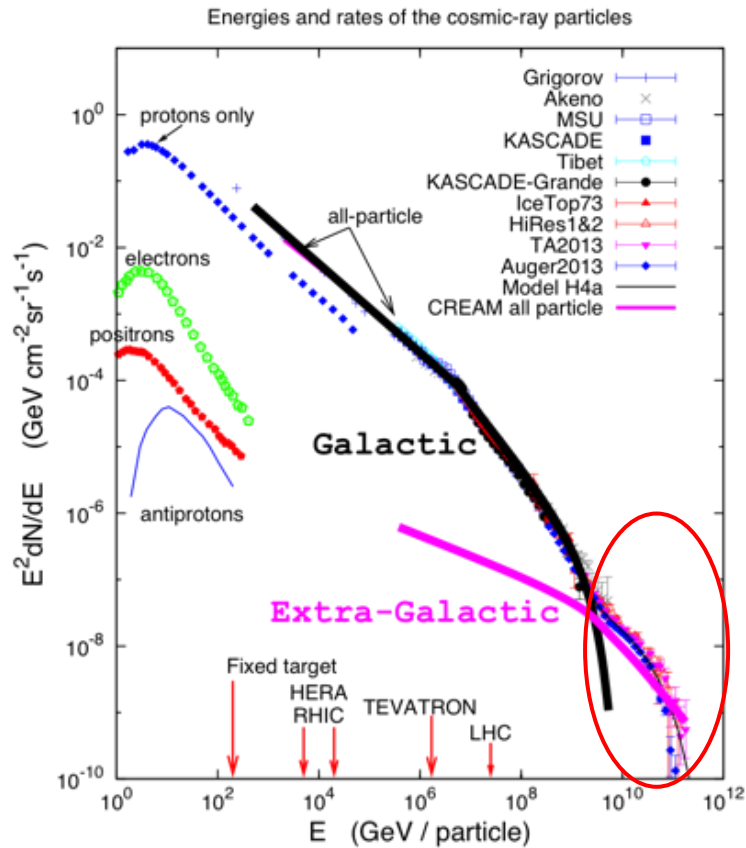


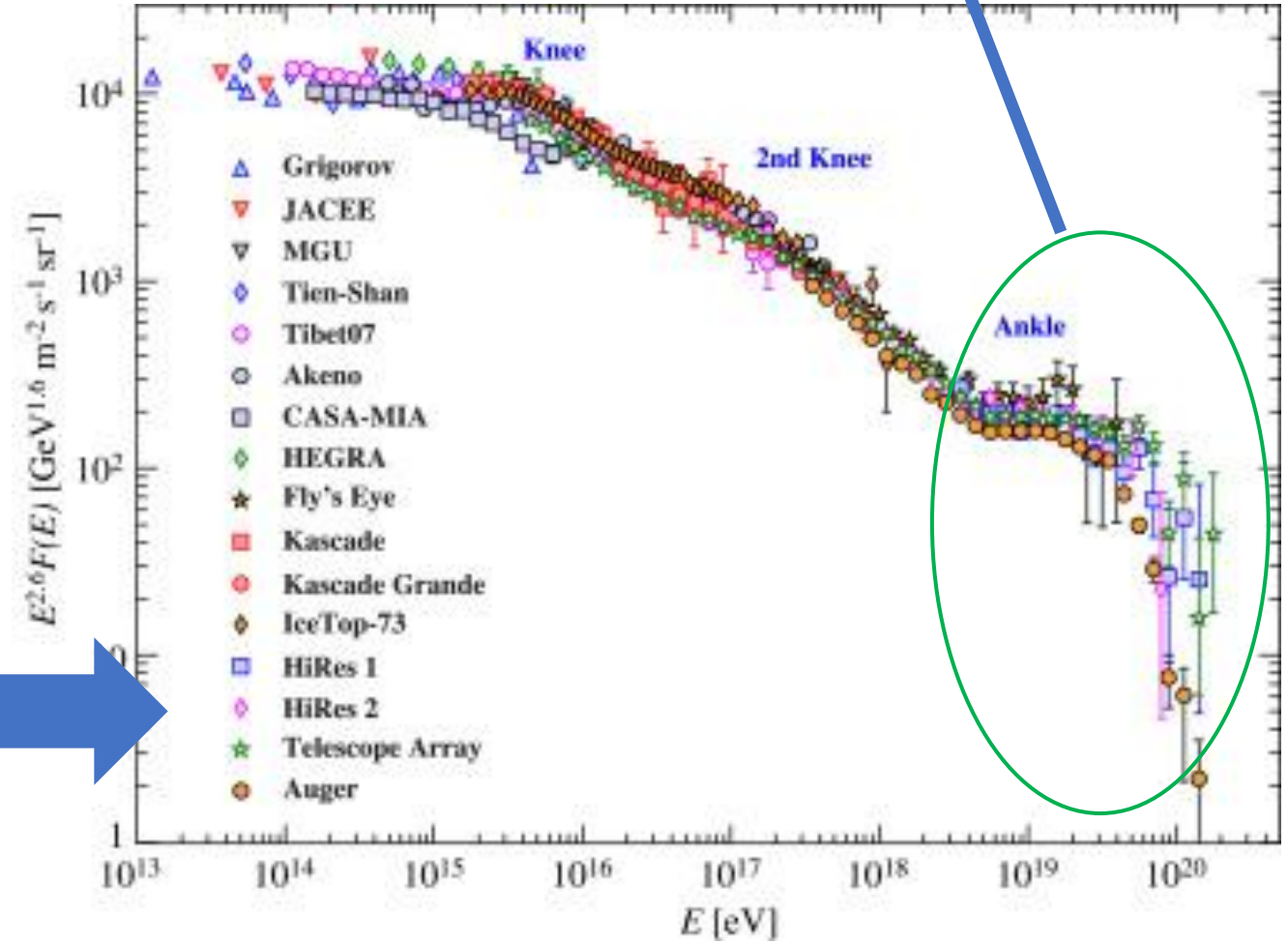
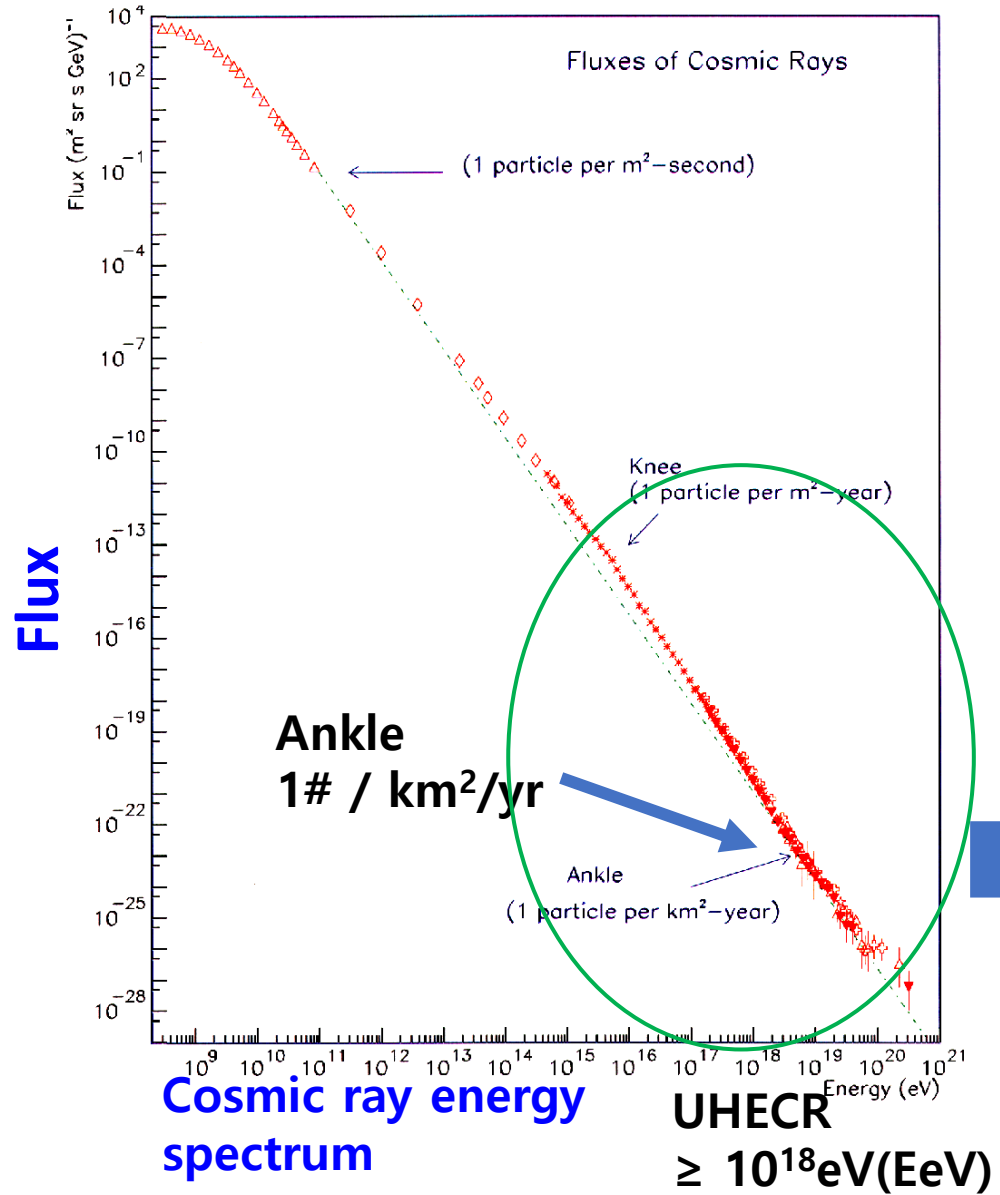
Ultra-High Energy Cosmic Rays Accelerated in FR Radio Galaxy Jets

Dongsu Ryu (UNIST, Ulsan, Korea)

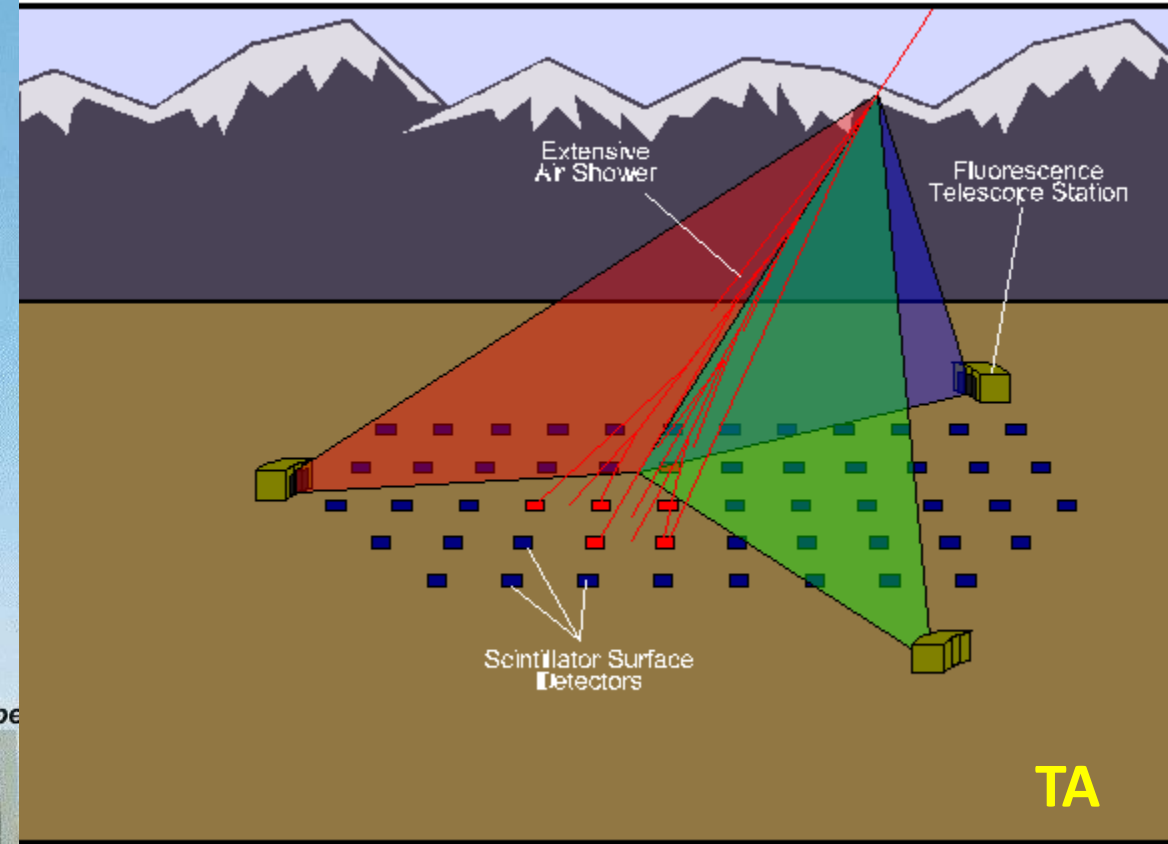
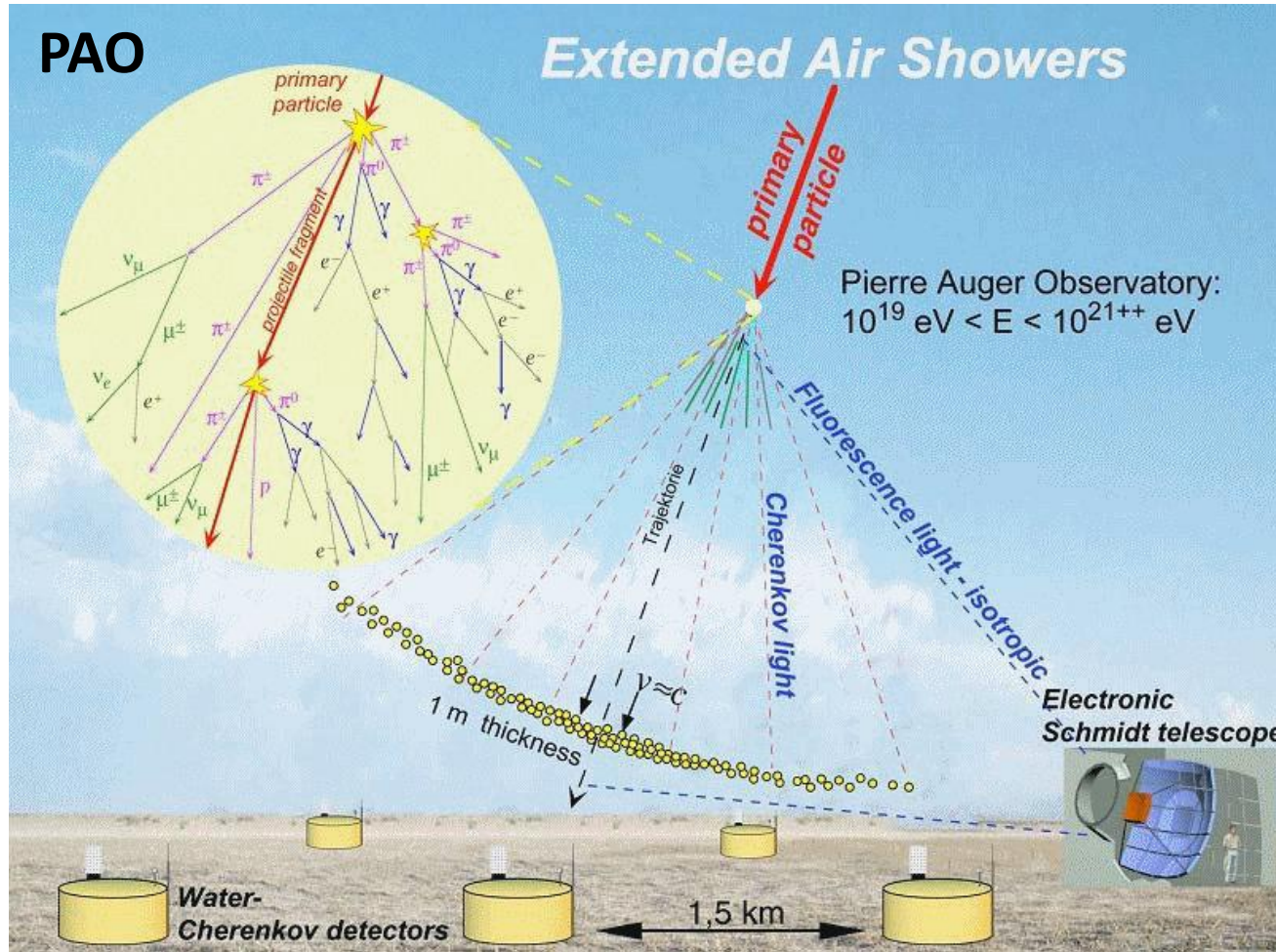
Hyesung Kang (Pusan National University, Korea) and Jeongbhin Seo (LANL, USA)



Observation of ultra-high energy cosmic rays (UHECRs)

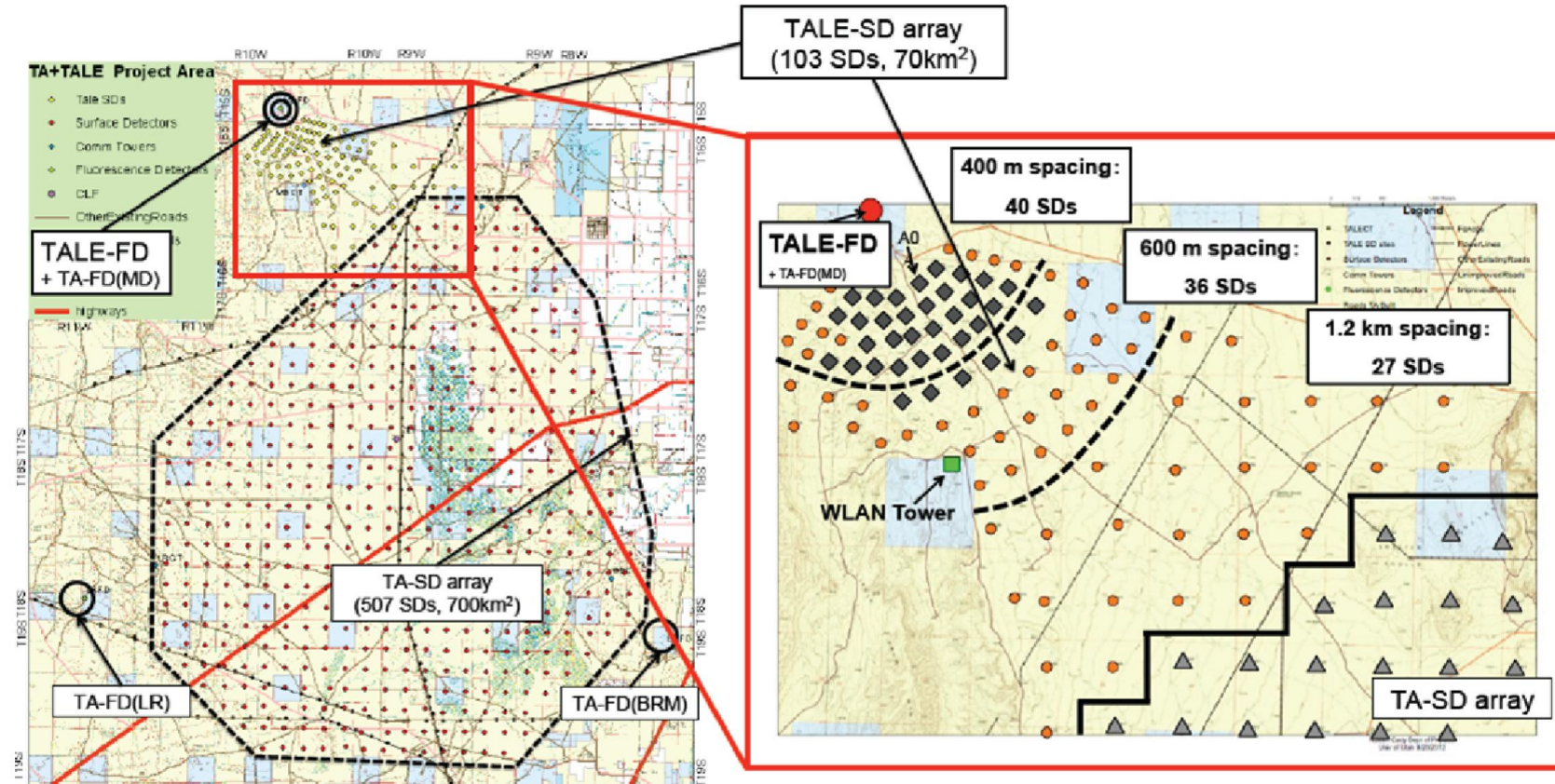
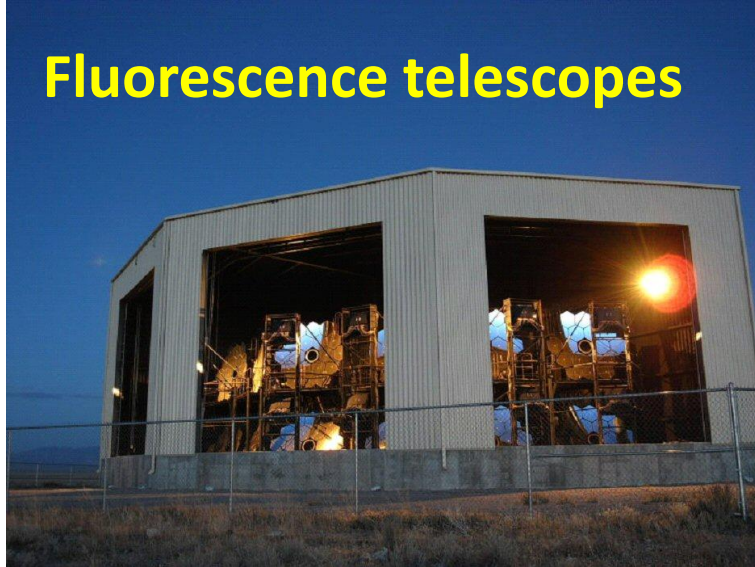


Observation of UHECRs: Extensive Air Shower (EAS)



Two leading experiments for observation of UHECRs

Telescope Array (TA) experiment in Delta, Utah, USA \longrightarrow Northern hemisphere



Japan, USA, Korea, & Russia

Two leading experiments for observation of UHECRs

Pierre Auger Observatory (PAO) in Argentina



Southern hemisphere



Location of Pierre Auger Observatory

Fluorescence telescopes

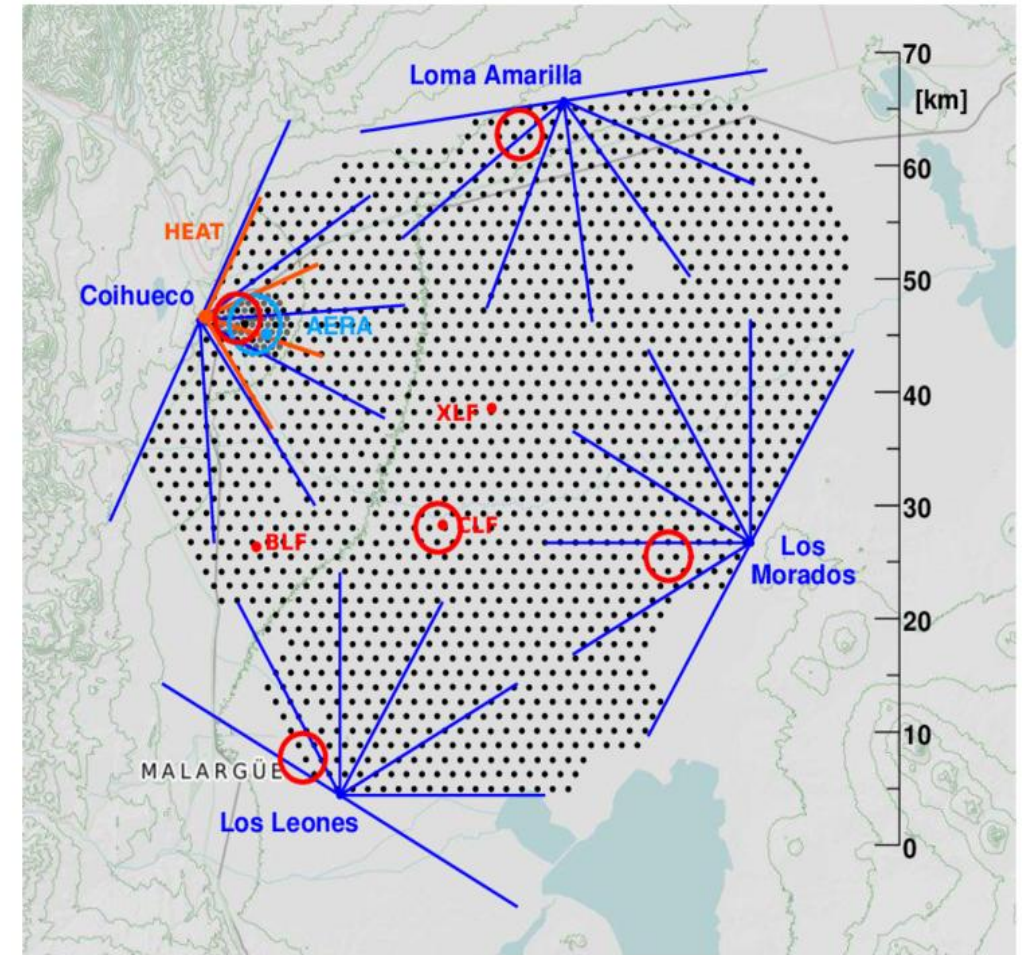


- Mirror surface: 3.6 m x 3.6 m (spherical)
- Opening: 30° x 30°
- Camera: 80 cm x 80 cm

Cherenkov detectors

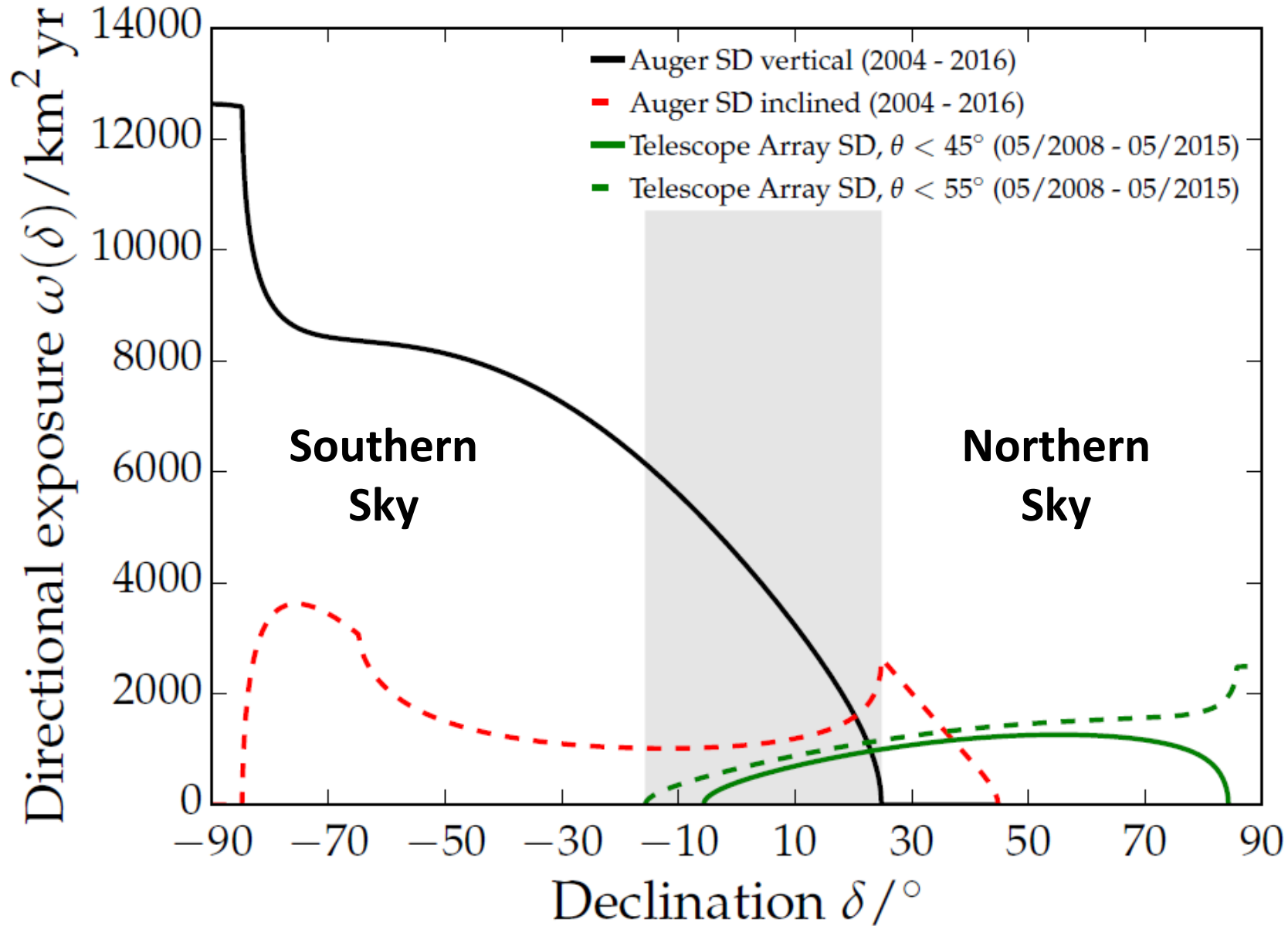


- Diameter: 3.6 m
- Water depth: 1.2 m
- Volume: 12 m³



Mostly European countries + Argentina

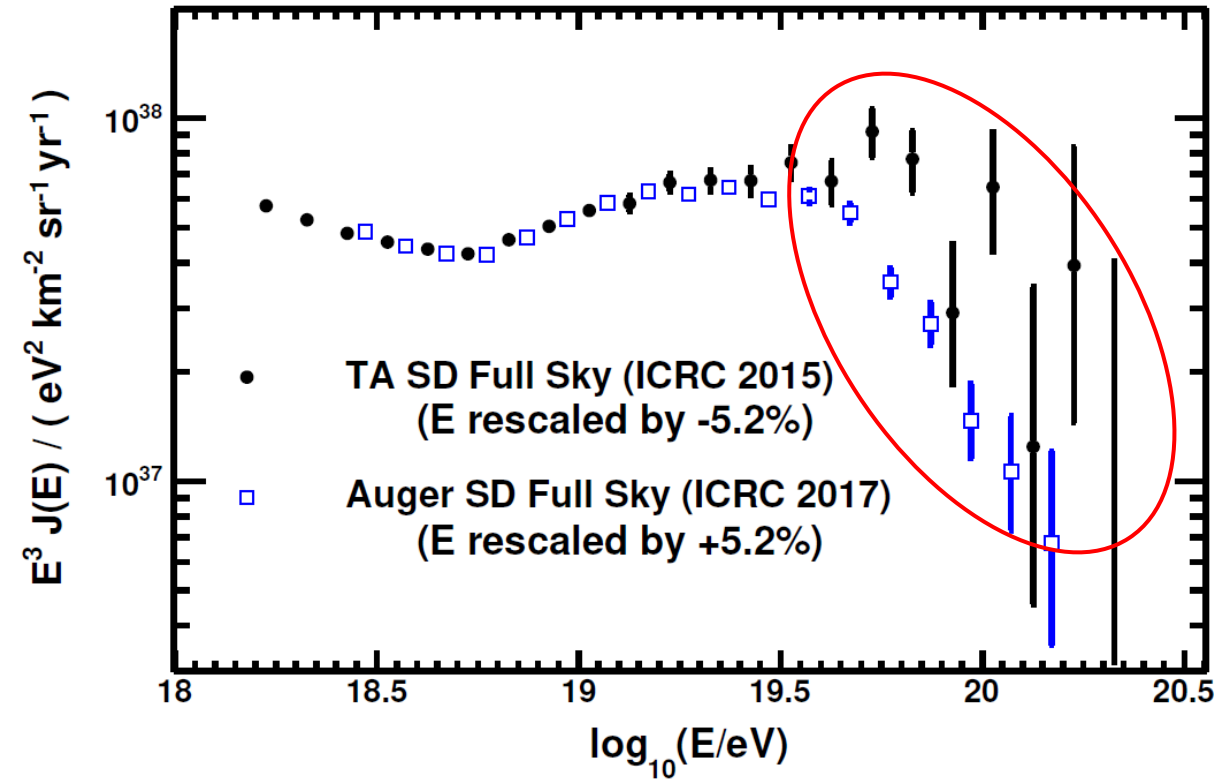
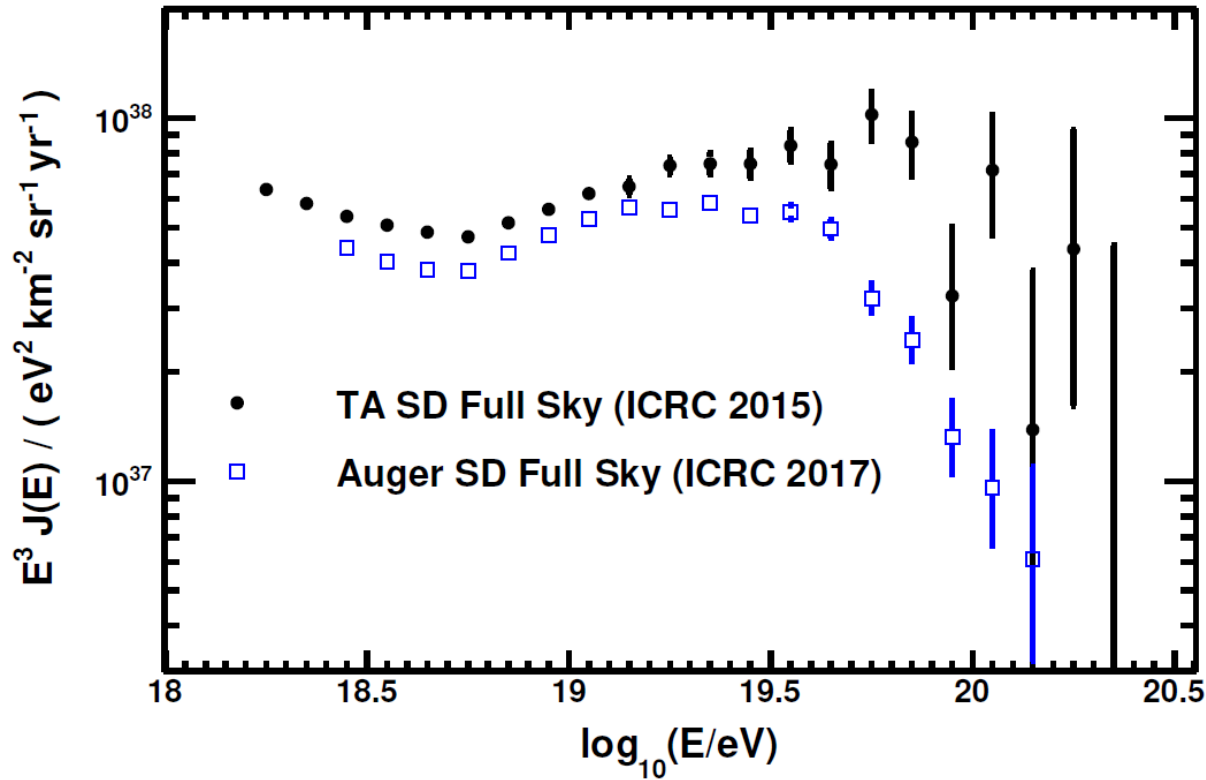
Sky coverage of two experiments



- **PAO** sees UHECRs coming through the **southern sky**
- **TA** sees UHECRs coming through the **northern sky**

Differences in UHECRs observed by two experiments

Energy spectrum of UHECRs

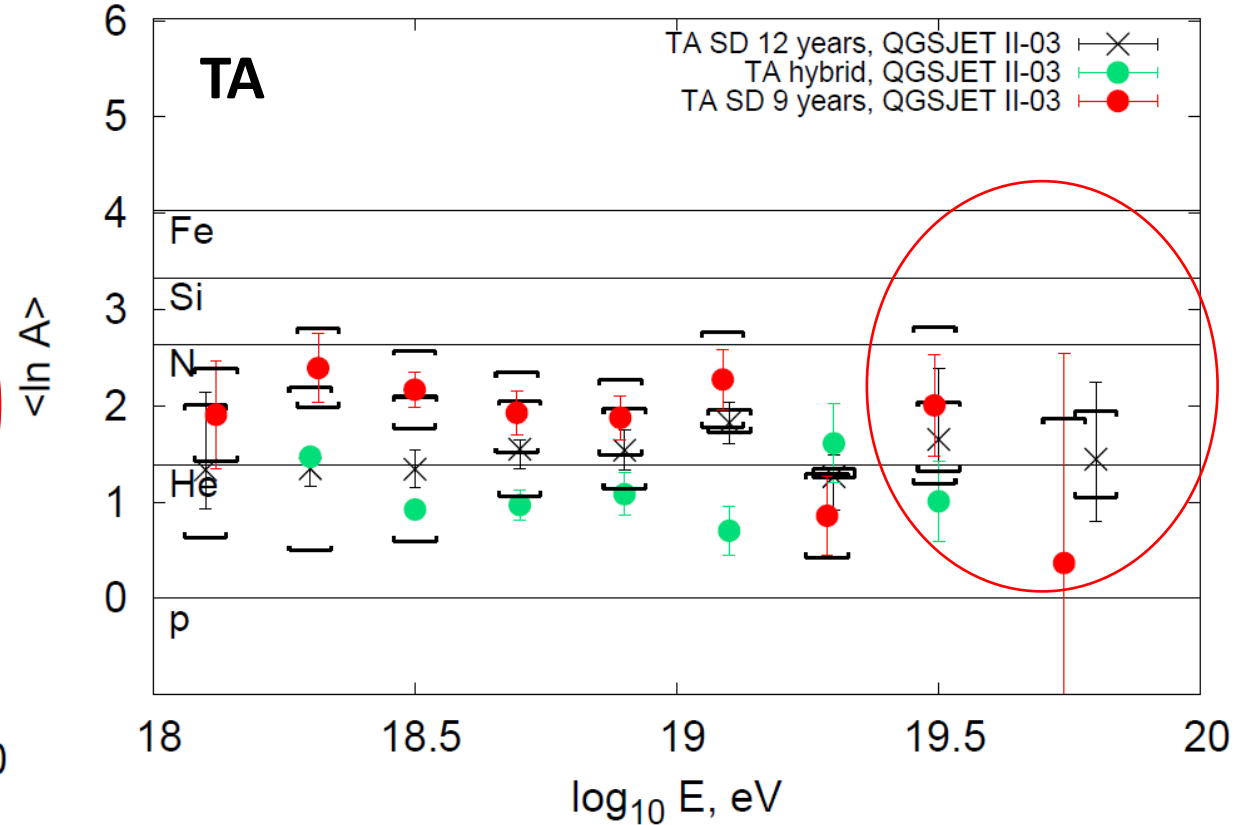
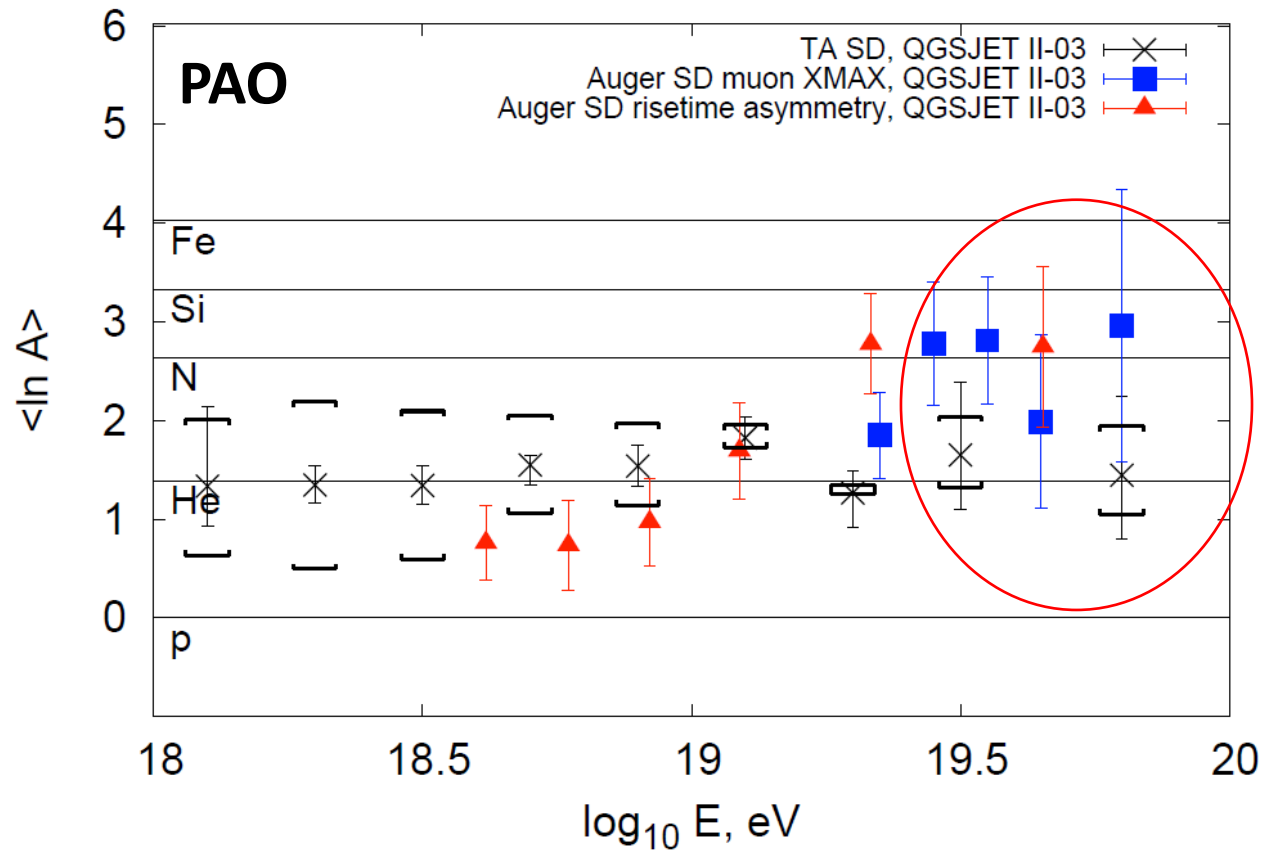


Flux of UHECRS with $E > \sim 3 \times 10^{19}$ eV is higher in the northern sky!

Differences in UHECRs observed by two experiments

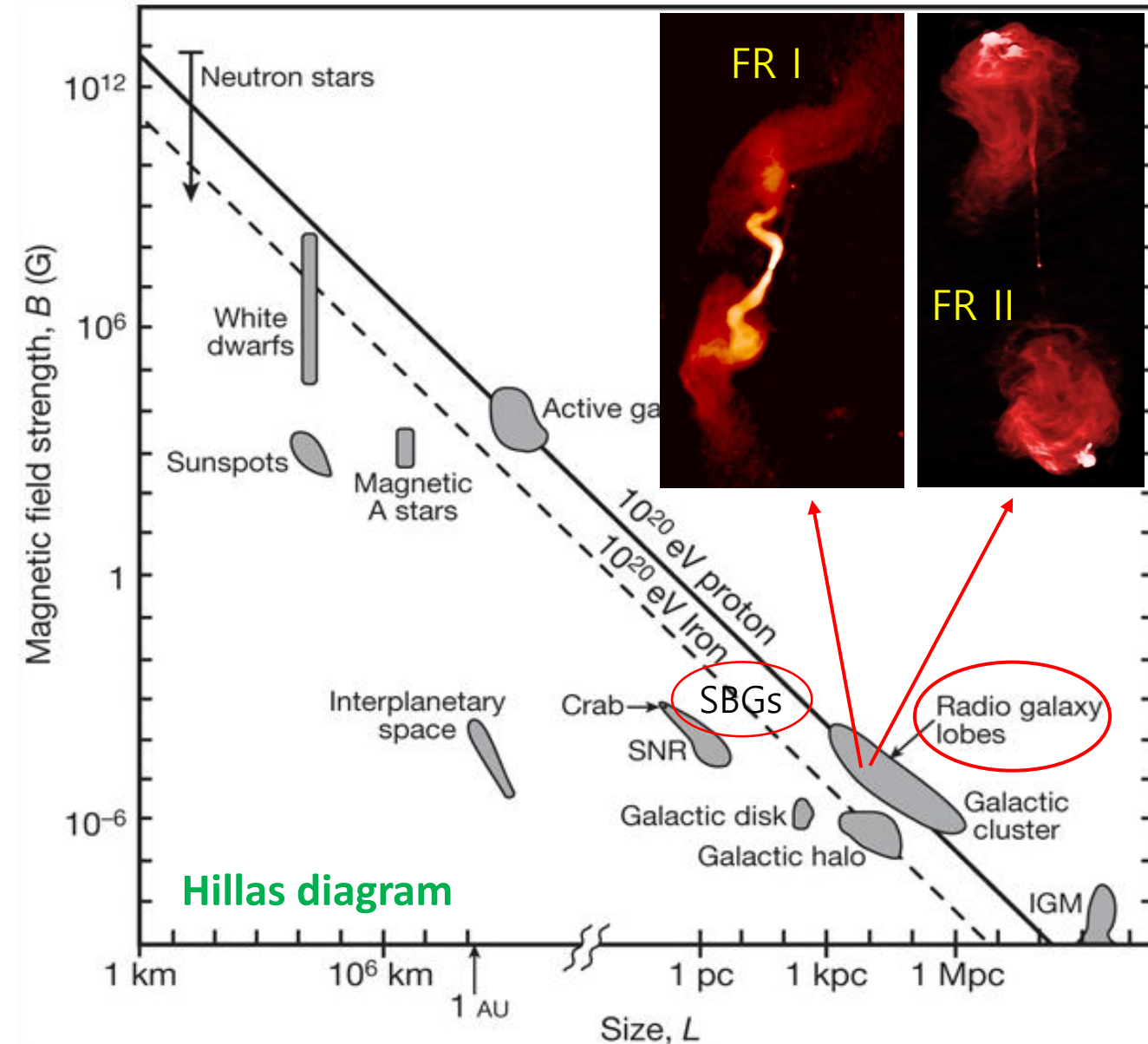
Mass composition of UHECRs

A: atomic mass



Mass of UHECRs with $E > \sim 3 \times 10^{19}$ eV is heavier in the northern sky!

Radio galaxies: possible astrophysical sources of UHECRs



Confinement condition ← Hillas criteria

Particles should be confined within $r_g \leq L$ accelerator in order to be accelerated.

→ $E_{Hillas}(EeV) \leq \beta_a \cdot B_{\mu G} L_{kpc}$ for proton

$E_{Z_i, Hillas} = Z_i E_{Hillas}$

Z_i charge $\beta_a = V_a/c$ $B_{\mu G} = \frac{B}{1\mu G}$ $L_{kpc} = \frac{L}{1kpc}$

Radio Galaxies (RGs):

FR-I : mildly relativistic jet, two-sided, plume-like

FR-II : highly relativistic jet, brighter lobed (hot spot), often one-sided (relativistic beaming)

Most promising candidate for UHECR sources ?

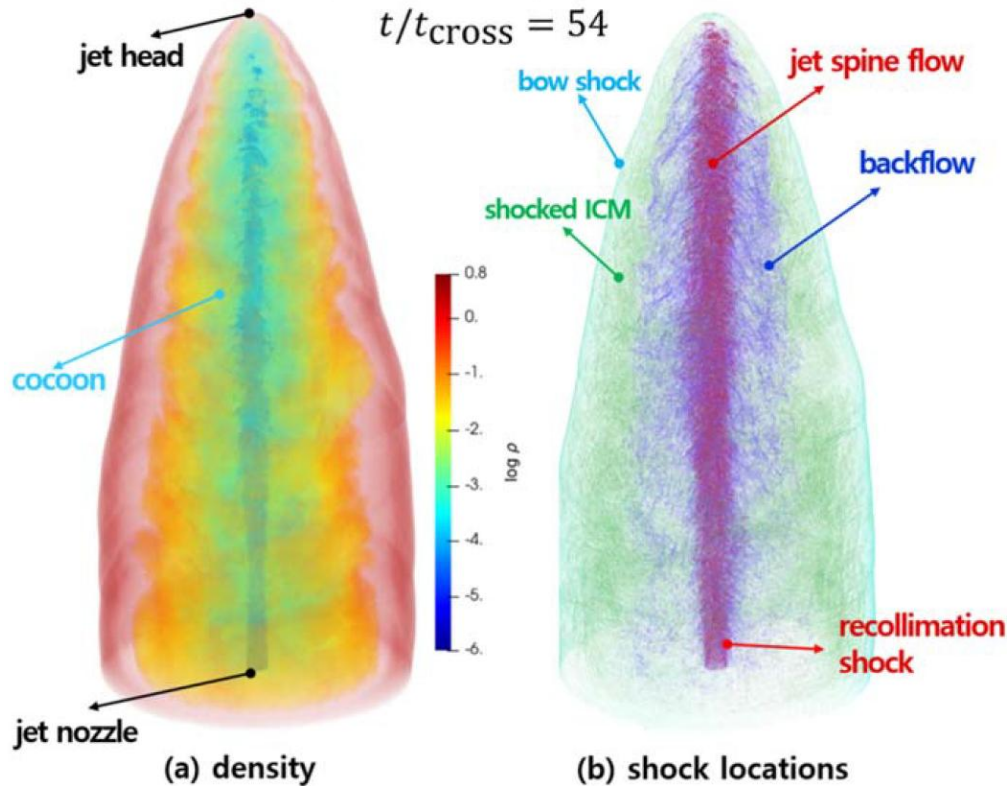
(Blandford et al. 2019; Rieger 2019; Hardcastle & Croston 2020; Matthews et al. 2020, + many previous studies)

Quantitative numerical estimation of UHECR spectrum from RG jets

3D Relativistic hydrodynamic (RHD) simulations for relativistic jets with $\Gamma_j \sim 1 - 100$ Seo et al. 2021b

adopt models for
 - B field amp
 - $\lambda_{\text{mfp}} \propto p^\delta$

Monte Carlo simulations of the CR transport in the simulated jet-induced flows.



Jet Parameters: $Q_j, r_j, \eta = \rho_j / \rho_b$, while $p_j = p_b$

Jet power: $Q_j = \pi r_j^2 v_j (\Gamma_j^2 \rho_j h_j - \Gamma_j \rho_j c^2)$

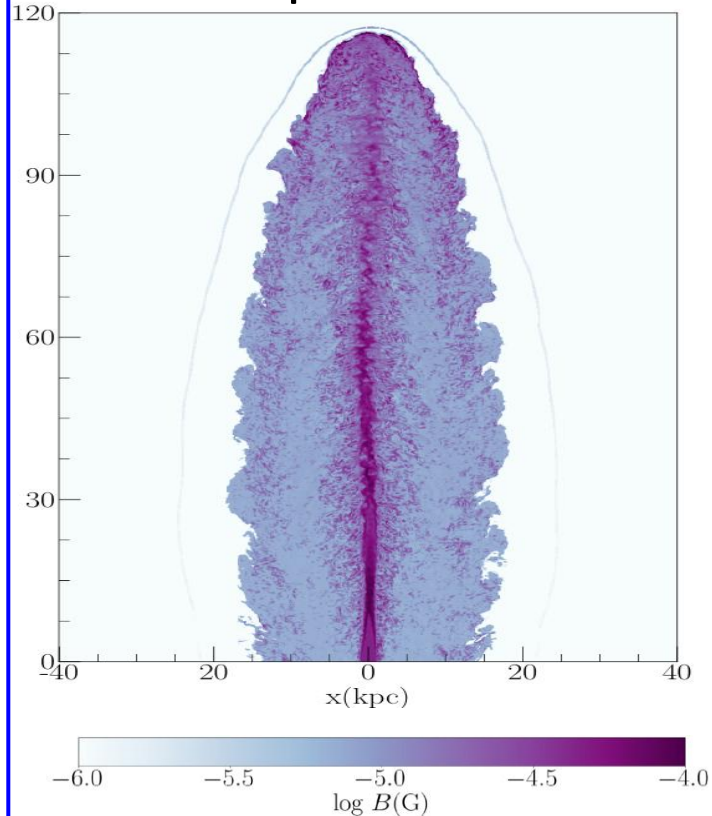
$r_j = 10 \text{ pc} - 1 \text{ kpc}, \Gamma_j \sim 1 - 100, Q_j \sim 10^{42} - 10^{47} \text{ erg/s}$

jet bulk **Lorentz factor** $\Gamma_j = \frac{1}{\sqrt{1 - \left(\frac{v_j}{c}\right)^2}} \propto \left(\frac{Q_j}{\rho_j \pi r^2}\right)^{1/2}$

Higher-power jets are more relativistic.

Monte Carlo simulations for CR transport

- Prescription for B fields



Jet spine: $B \sim 100\mu\text{G}$
Backflow: $B \sim 10\mu\text{G}$
ICM: $B \sim 1\mu\text{G}$

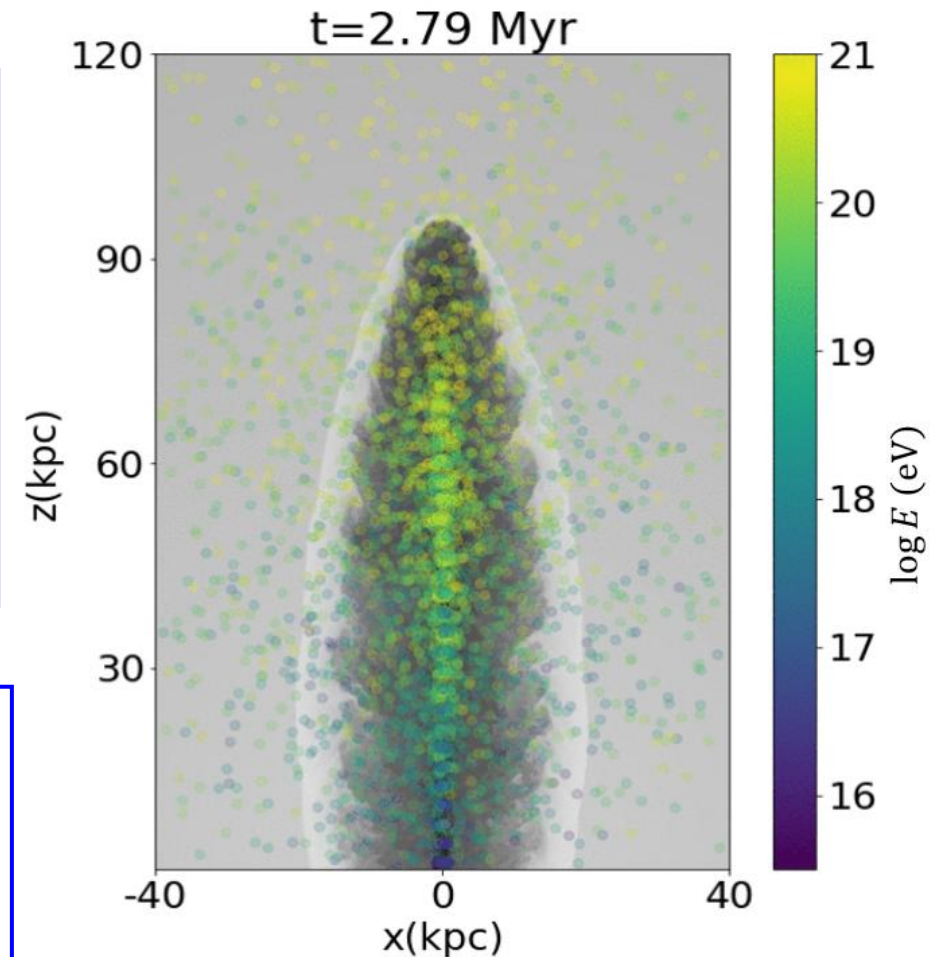
- MHD turbulence, $\frac{\delta B}{B}$,
on subgrid scales
 $\lambda_{\text{mfp}} \propto E^\delta$
 $\delta = 1$ for Bohm
 $\delta = 1/3$ for Kolmogorov

- Galactic CR seeds

$$dN/dE \propto E^{-2.7}$$

with $E = 10^{13} - 10^{15}$ eV

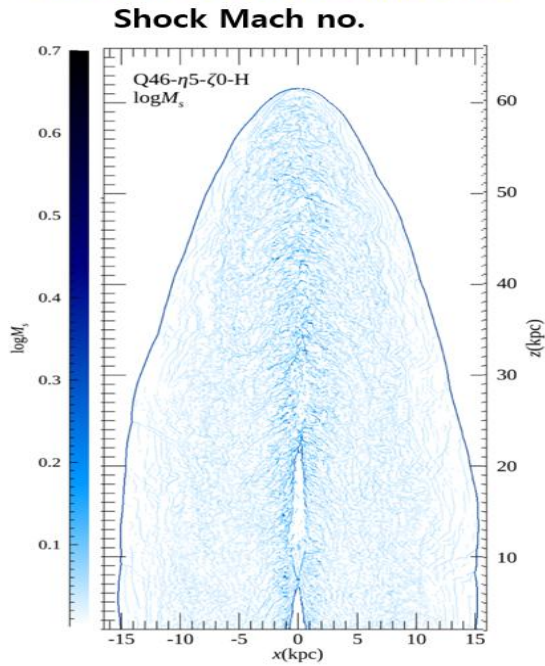
injected from the host galaxy
through the jet nozzle



Particles are advected & energized
by **shocks, shear, and turbulence**
in the time-evolving jet flows.

Three Main Particle Acceleration Mechanisms

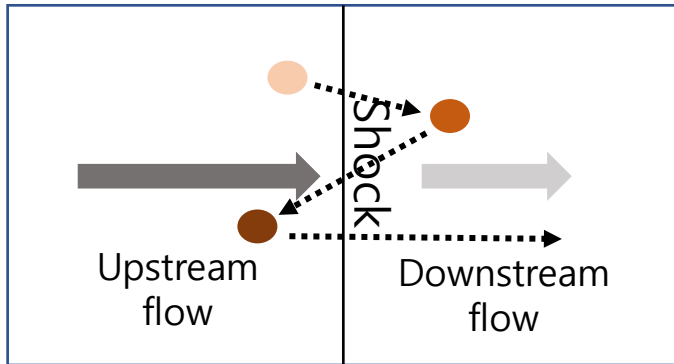
Diffusive Shock Acceleration



steep spectrum

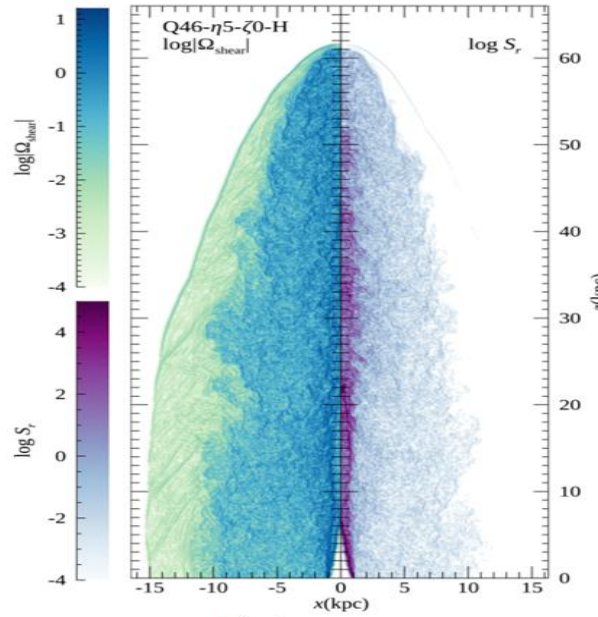
$$dN/dE \propto E^{-\sigma} \quad \sigma = (\chi + 2)/(\chi - 1)$$

$\chi = \rho_2/\rho_1$ compression ratio of the shock



Shear Acceleration

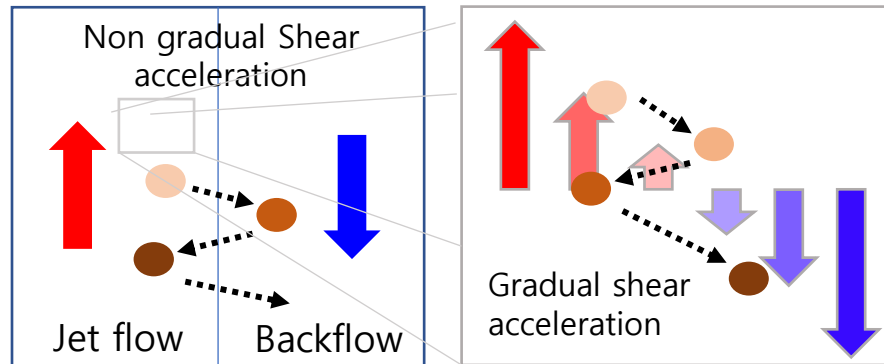
Relativistic shear coefficient



$$S_r = \frac{\Gamma_v^4}{15} \left(\frac{\partial v_z}{\partial r} \right)^2, \quad \text{flat spectrum}$$

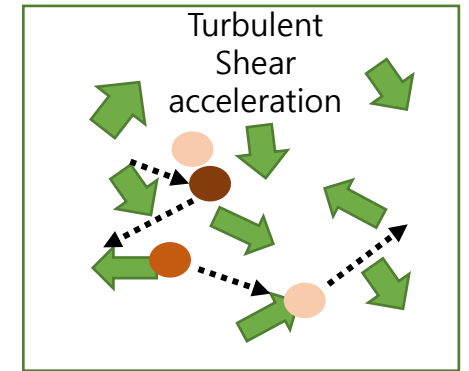
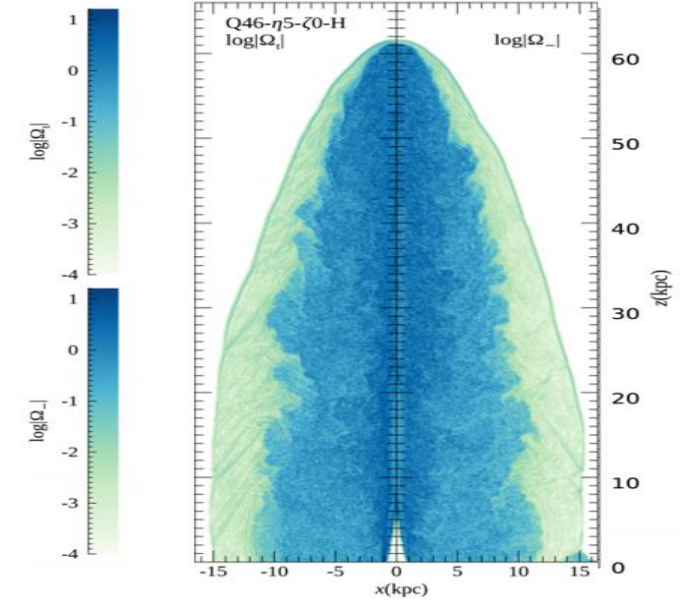
$$dN/dE = 4\pi p^2 f(p) \propto E^{-1+\delta}, \quad \tau(p) \propto p^\delta$$

$$dN/dE \propto E^0 \text{ for the Bohm diffusion}$$

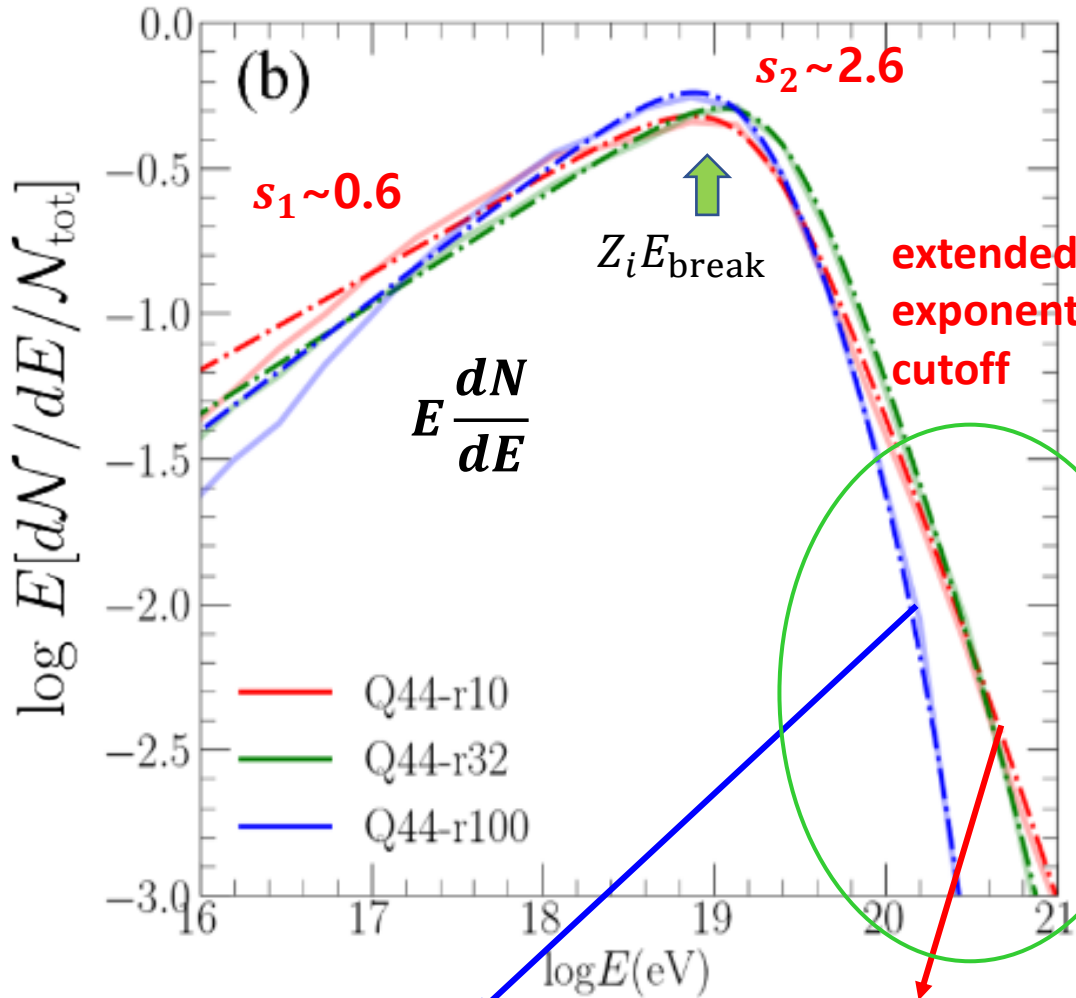


Turbulent Acceleration

Vorticity = turbulence



Energy spectrum of CR particles escaping from the jets



double power law with an extended exponential cutoff

Seo et al 2024

$$\frac{dN}{dE} \propto \left(\left(\frac{E}{Z_i E_{\text{break}}} \right)^{-s_1} + \left(\frac{E}{Z_i E_{\text{break}}} \right)^{-s_2} \right)^{-1} \times \exp \left(- \frac{E}{Z_i E_{\text{break}} \langle \Gamma \rangle_{\text{spine}}^2} \right)$$

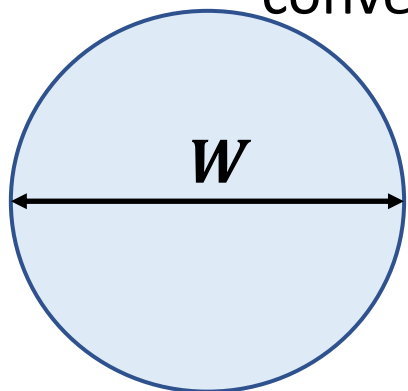
- $s_1 \sim 0.6$ & $s_2 \sim 2.6$
- $Z_i E_{\text{break}}$: depends mainly on $\left(\frac{Q_j}{\pi r^2} \right)$
- exponential cutoff at $Z_i E_{\text{break}} \langle \Gamma \rangle_{\text{spine}}^2$
- $\langle \Gamma \rangle_{\text{spine}}$: mean Lorentz factor of jet-spine flow

mildly relativistic jet
 $\Gamma_j = 3.9, \langle \Gamma \rangle_{\text{spine}} \sim 2.7$

relativistic jet
 $\langle \Gamma \rangle_{\text{spine}} \sim 5.8$
 $\Gamma_j = 11$

Why double power law with an extended exponential cutoff

conventional single power law with a cutoff



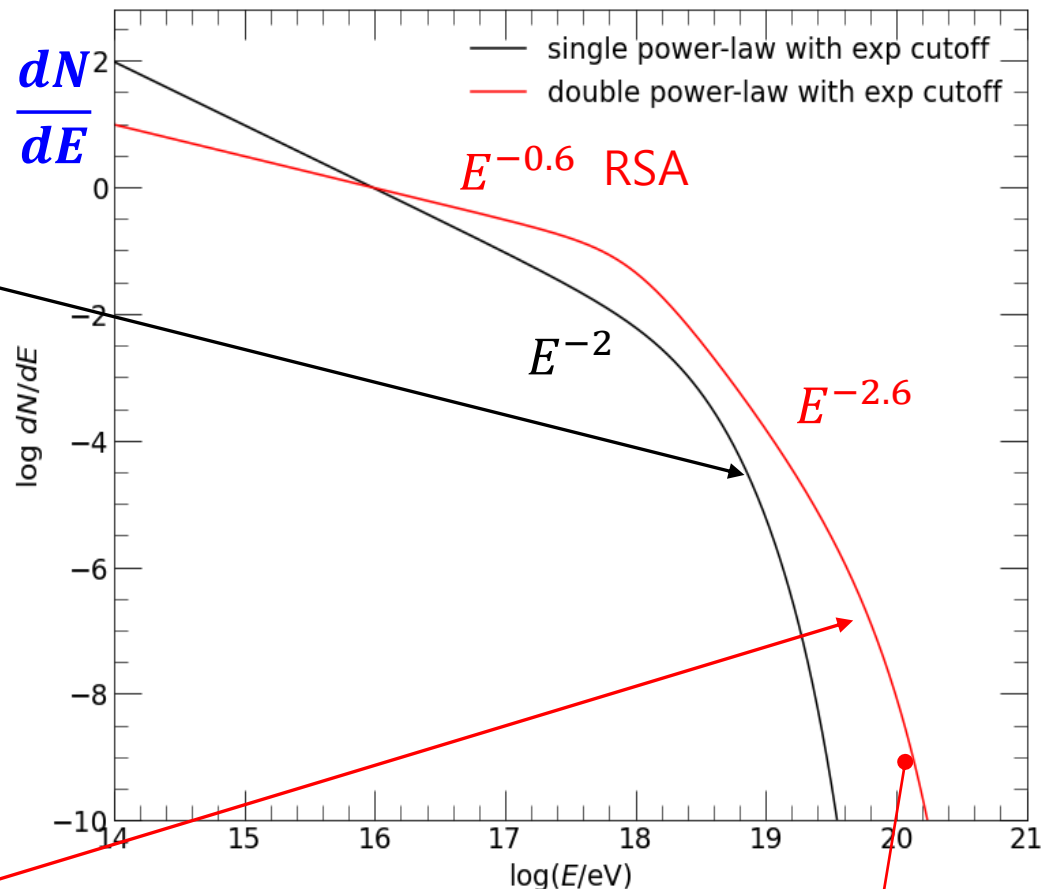
$$\frac{dN}{dE} \propto E^{-2}$$

DSA power law

$$E_{\text{break}} \sim E_H \approx 0.9 \text{ EeV} \left(\frac{\langle B \rangle}{1 \mu\text{G}} \right) \left(\frac{0.5W}{1 \text{ kpc}} \right)$$

$$\frac{dN}{dE}$$

$\log dN/dE$



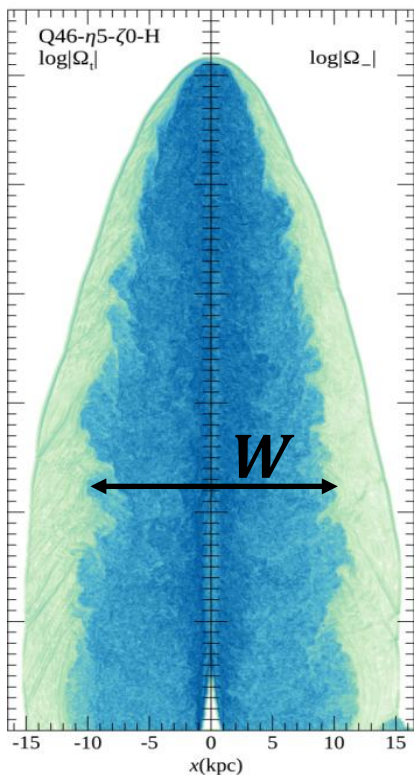
• $E < Z_i E_{\text{break}} : dN/dE \propto E^{-0.6}$
 due to relativistic shear acceleration
 cf. Ostrowski 1998
 Kimura et al 2018

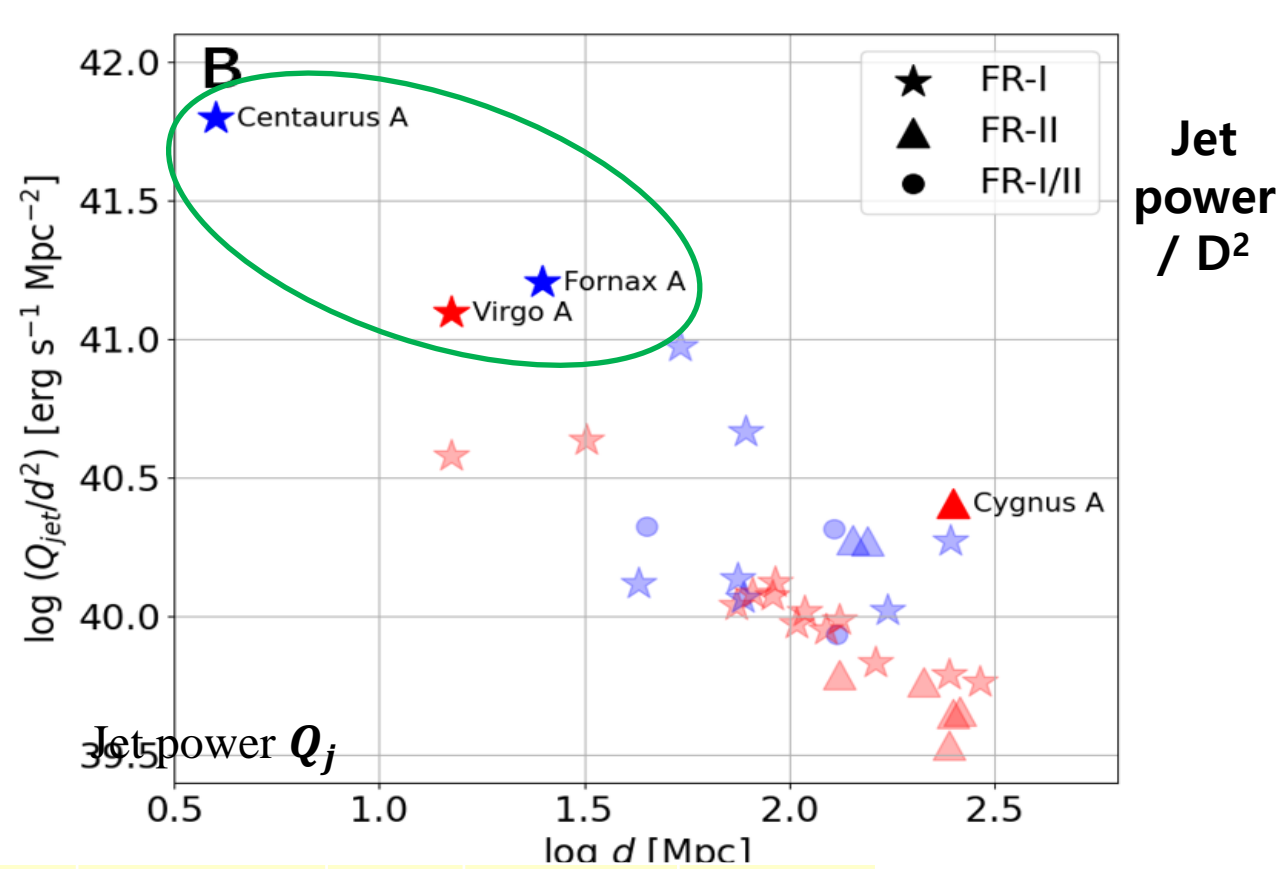
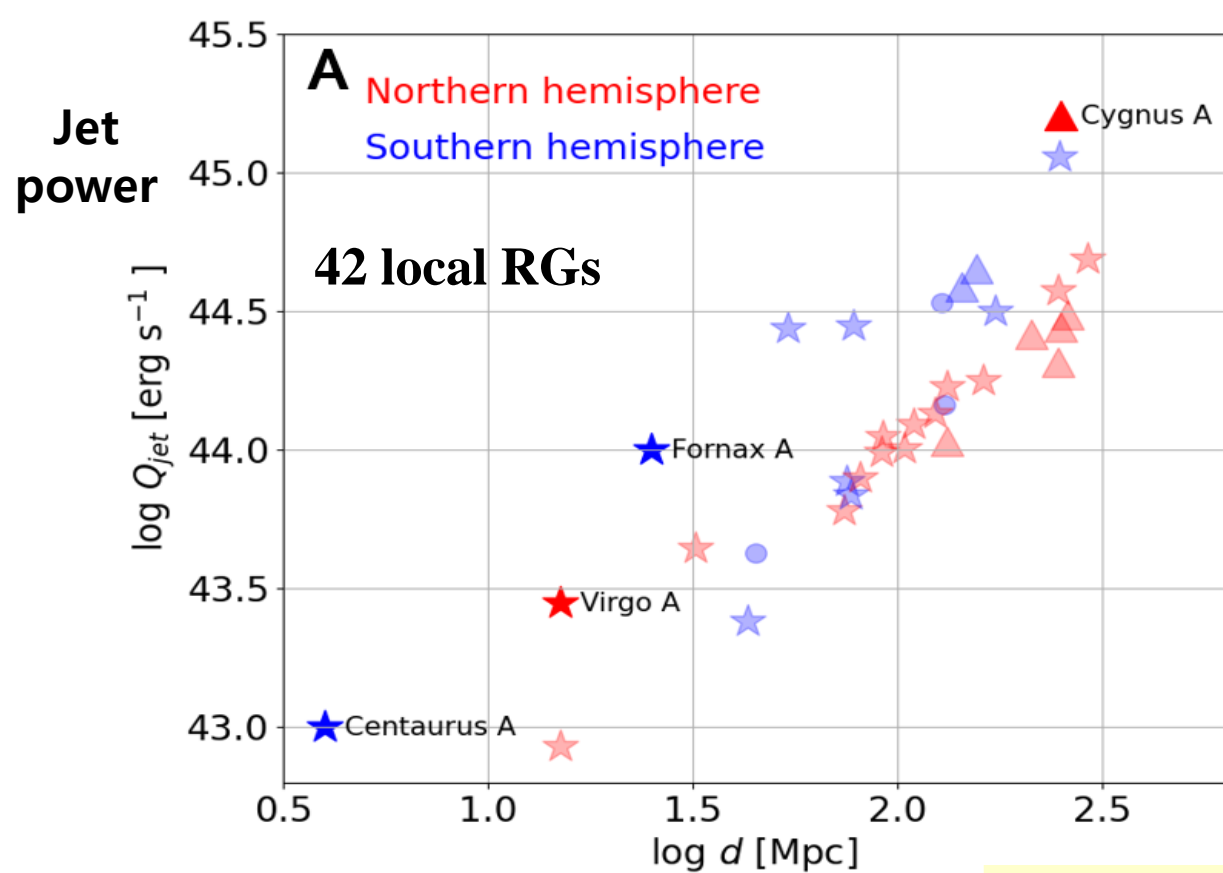
Elongated cylinder (cocoon)
 double power-law with a cutoff

• $E > Z_i E_{\text{break}} : dN/dE \propto E^{-2.6}$
 controlled by the confinement within
 an elongated cocoon

**Non-gradual shear
 acceleration**

$$E_{\text{cutoff}} \sim Z_i E_{\text{break}} \langle \Gamma \rangle_{\text{spine}}^2$$





TA: dominant source of northern sky
 → Virgo A

Auger: important sources of southern sky
 → Centaurus A & Fornax A

Name	Q_j (erg/s)	Γ_j	E_b (Eev)	d (Mpc)
Virgo A	2.5E43	7.0	10.5	16
Cygnus A	1.5E45	10.0	51.2	250
Centaurus A	1.0E43	1.2	2.8	4
Fornax A	1.0E44	1.5	6.6	25

UHECRs keep losing energy & disintegrated during propagation !

Application of our model spectrum to reproduce observations of UHECRs

- Model Source Spectrum at RGs

Seo et al. 2025

$$\frac{dN}{dEdt} \propto \left(\left(\frac{E}{ZE_b} \right)^{-s_1} + \left(\frac{E}{ZE_b} \right)^{-s_2} \right)^{-1} \exp \left(- \frac{E}{\langle \Gamma_j \rangle^2 ZE_b} \right)$$

E & Z : energy & charge of the particle

$s_1 \approx 0.6$ & $s_2 \approx 2.6$ $\langle \Gamma_j \rangle$: Lorentz factor of the jet

Model for Break energy: $E_b(Q_j) = \xi\varphi \cdot E_H \cdot (Q_j/Q_n)^\alpha$

based on our RHD &
MC simulation results

$$Q_n \approx 3.5 \times 10^{44} \text{ erg/s}, \quad E_H \approx 4.5 \times 10^{19} \text{ eV},$$

$$\alpha \approx 1/4 \text{ for FR-I} \quad \& \quad \alpha \approx 1/3 \text{ for FR-II},$$

$$\xi\varphi \sim 0.15 - 0.7 \text{ (depending on } \langle \Gamma_j \rangle \text{)}$$

different $\langle \Gamma_j \rangle$ for different RGs, based on observations

- Chemical abundance: 3 x Galactic abundance for hosting elliptical galaxies

Propagation of UHECRs from RGs to Earth



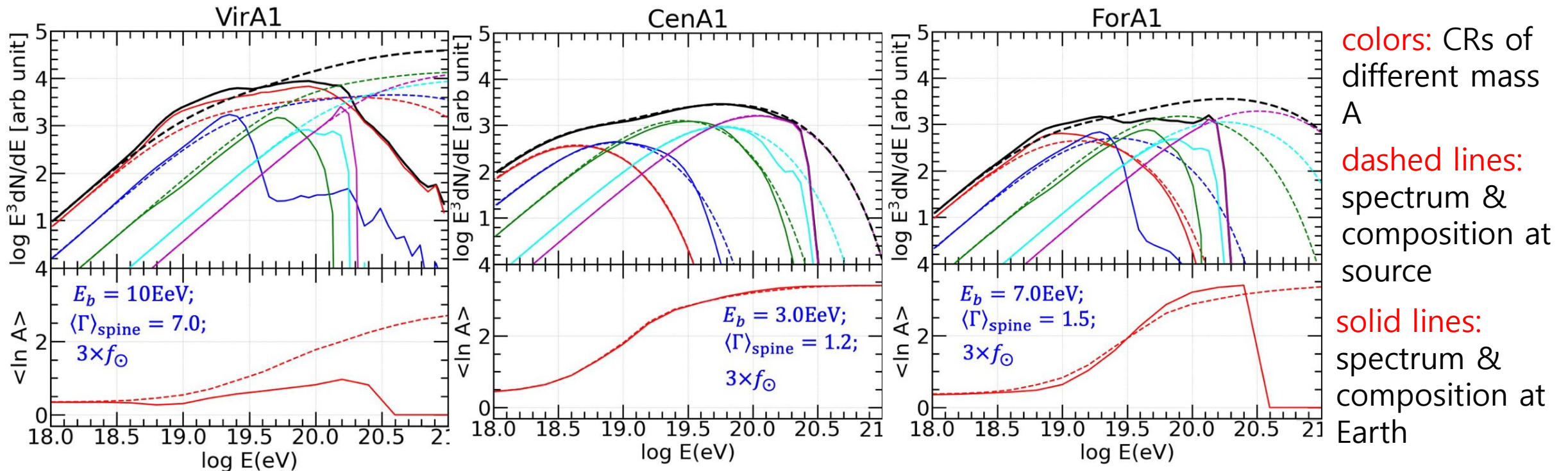
<https://crpropa.desy.de/>

R. Alves Batista, et al. 2022

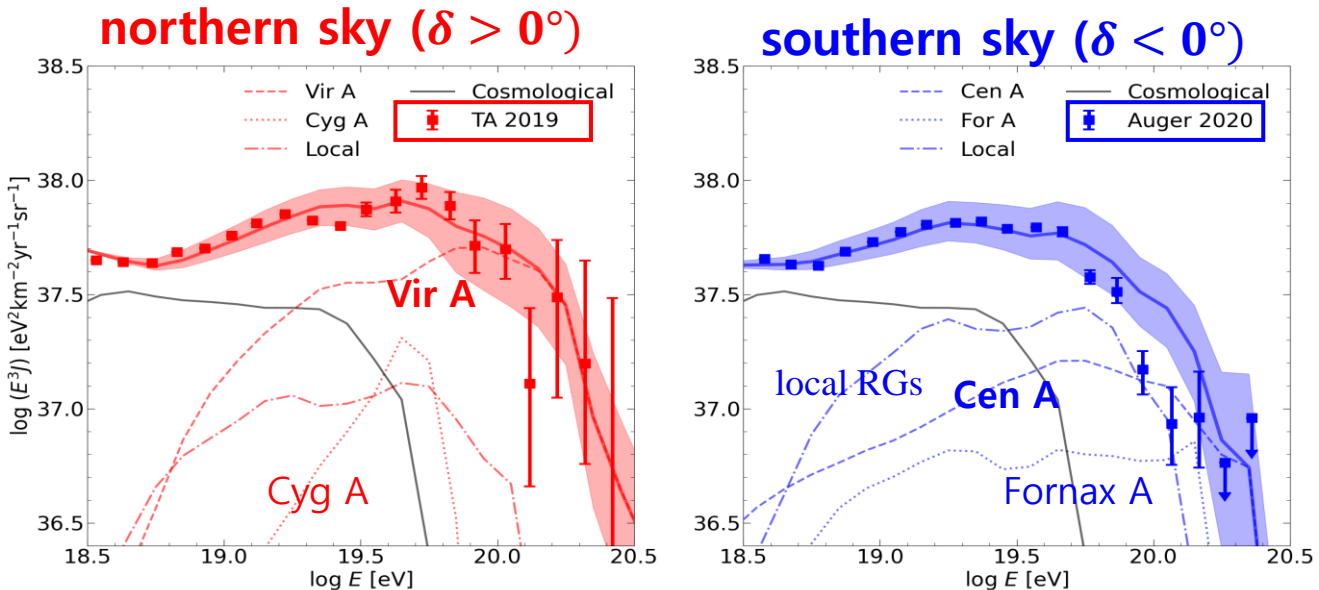
In **CRPropa3** simulations, we include the following modules:

- photo-pion Production
- photodisintegration
- electron pair production by CMB and extragalactic background light (Gilmore et al. 2012)
- redshift evolution (adiabatic energy loss)

$$d_{\text{prop}} \sim 1 - 1.5 d_{RG}$$

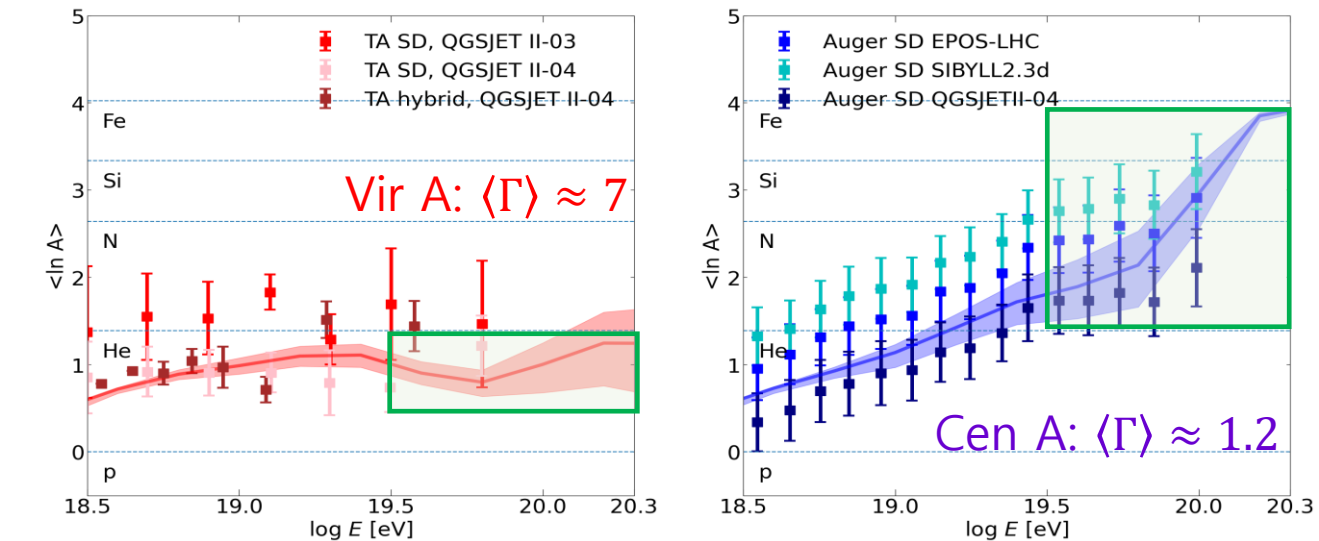


Energy spectrum & mass composition of UHECRs from radio galaxy jets



- **Virgo A with $\langle \Gamma \rangle \sim 7$** is the dominant source in the northern hemisphere.
- **Cen A with $\langle \Gamma \rangle \sim 1.2$** and other **local RGs** are dominant sources in the southern hemisphere.
- **RGs with larger $\langle \Gamma \rangle$** result in lighter mass composition, i.e., smaller $\langle \ln A \rangle$, of UHECRs with $E > 10^{19}$ eV.

Seo et al. 2025



Shading represents $\pm 20\%$ variations of model parameters.

Summary

1. The energy spectrum of UHECRs produced at radio galaxies (RGs) can be modeled as a double power law with an extended exponential cutoff.
2. Our source spectrum model suggests an observed UHECR spectrum that may extend to higher energies and exhibits a lighter mass composition, $\langle \ln A \rangle$, at the highest energies.
3. RGs in the local universe, including **Virgo A**, **Cen A**, and **Fornax A**, could be the primary sources of UHECRs. **Virgo A**, with its more relativistic jet, can generate a higher flux & a lighter composition at the highest end of the energy spectrum in the northern hemisphere, compared to those in the southern hemisphere.
4. Our model could explain the observed differences in the energy spectrum and mass composition of UHECRs between the northern and southern hemispheres. e.g., TA versus PAO.
5. Anisotropy in the observed directions of UHECRs is another important properties. To explain it, we need the distribution of magnetic fields in the local universe as well as in our galaxy.

